Articles

Four- and Five-Coordinate CO Insertion in the Copolymerization of Carbon Monoxide and Olefins Catalyzed by Diphosphine Nickel(II) Complexes: A Dynamical Density Functional Study

Filippo De Angelis and Antonio Sgamellotti*

Istituto CNR di Scienze e Tecnologie Molecolari c/o Dipartimento di Chimica, Università di Perugia, I-06123 Perugia, Italy

Nazzareno Re

Facoltà di Farmacia, Università G. D'Annunzio, I-06100 Chieti, Italy

Received December 3, 2001

We have carried out a theoretical study of the migratory insertion step in the cationic Ni(II) $[(dppp)Ni(CH_3)(CO)]^+$ complex by means of both static and dynamic density functional methods to shed light on the mechanistic aspects of the migratory insertion and in particular on the role played by five-coordinate species. We find the addition−insertion pathway, taking place via a five-coordinate complex, to be thermodynamically and kinetically favored, with a highest energy barrier of 7.9 kcal mol^{-1}, in agreement with the experimental data. Dynamics simulations have shown that the migratory insertion reaction takes place by a methyl attack on the resting carbonyl group.

Introduction

Copolymerization of carbon monoxide and olefins has attracted much attention because of the useful chemical and physical properties of the resulting copolymers.[1−3] This process is catalyzed by cationic Pd(II) systems employing bidentate phosphine ligands, such as 1,3-bis-(diphenylphosphino)propane, $(C_6H_5)_2P(CH_2)_3P(C_6H_5)_2$ (dppp). The catalytically active species is thought to be a d^8 square-planar cationic palladium complex $[(L-L)-Pd(II)P]^+$, where L−L represents the bidentate ligand and P the growing polymer chain, which successively undergo the two alternating propagation steps: (i) CO migratory insertion into an alkyl−Pd bond and (ii) olefin migratory insertion into an acyl−Pd bond. These migratory insertion reactions are members of a larger class of migratory insertion reactions that constitute key steps of transition metal catalyzed C−C bond-forming reactions.[4] Of these reactions, the alkyl migration to CO is probably the most completely examined both from an experimental[4] and theoretical point of view.[5] The migratory insertion of carbonyl alkyl complexes at a Pd(II) cationic center has been examined in detail,[6−9] and all experimental evidence indicates that no five-coordinated species are involved either as intermediates or as transition states in the CO migratory insertion step.

Ni(II) complexes have found little success in CO olefin copolymerization since they exhibit only modest activity;[10−13] however, cationic Ni(II) species based on the 1,2-bis(bis(2-methoxyphenyl)phosphino)ethane (o-MeO-dppe) ligand showed improved activity.[13] Brookhart and co-workers[14] have recently investigated the mechanism of CO ethylene copolymerization in a series of Ni(II) cationic diphosphine complexes. They identified several five-coordinate intermediates at variance with the analogous palladium systems, where four-coordinate species are the rule. In particular, the reaction of [(L−

(1) Sen, A. *Acc. Chem. Res.* **1993**, *26*, 303.
(2) Drent, E.; van Broekhaven, J. A. M.; Doyle, M. J. *J. Organomet. Chem.* **1991**, *417*, 235.
(3) Sen, A. *Adv. Polym. Sci.* **1986**, *73/74*, 125. Sen, A.; Jiang, Z.; Chen, J.-T. *Macromolecules* **1989**, *22*, 2012. Siddharth, S.; Jiang, Z.; Sen, A. *Polym. Prepr.* **1993**, *34*, 378.
(4) Collman, J. P.; Hegedus, L. S.; Norton, J. R.; Finke, R. G. *Principles and Applications of Organotransition Metal Chemistry*; University Science Books: Mill Valley, CA, 1987. Colquhoun, H. M.; Thompson, D. J.; Twigg, M. V. *Carbonylation, Direct Synthesis of Carbonyl Compounds*; Plenum Press: New York, 1991. Parshall, G. W.; Ittel, S. D. *Homogeneous Catalysis*, 2nd ed.; Wiley: New York, 1992.
(5) (a) Koga, N.; Morokuma, K. *J. Am. Chem. Soc.* **1985**, *107*, 7230. (b) Koga, N.; Morokuma, K. *J. Am. Chem. Soc.* **1986**, *108*, 6136. (c) Ziegler, T.; Versluis, L.; Tschinke, J. *J. Am. Chem. Soc.* **1986**, *108*, 612. (d) Bernardi, F.; Bottoni, A.; Nicastro, M.; Rossi, I.; Novoa, J.; Prat, X. *Organometallics* **2000**, *19*, 2170.
(6) Rix, F. C.; Brookhart, M. *J. Am. Chem. Soc.* **1995**, *117*, 1137.
(7) Rix, F. C.; Brookhart, M.; White, P. S. *J. Am. Chem. Soc.* **1996**, *118*, 4746.
(8) Shultz, C. S.; Ledford, J.; DeSimone, J. M.; Brookhart, M. *J. Am. Chem. Soc.* **2000**, *122*, 6351.
(9) Toth, I.; Elsevier, C. J. *J. Am. Chem. Soc.* **1993**, *115*, 10388.
(10) Klabunde, U.; Ittel, S. D. *J. Mol. Catal.* **1987**, *41*, 123.
(11) Desjardins, S. Y.; Cavell, K. J.; Hoare, J. L.; Skelton, B. W.; Sobolev, A. N.; White, A. H.; Keim, W. *J. Organomet. Chem.* **1997**, *544*, 163.
(12) Domhöver, B.; Kläui, W.; Kremer-Aach, A.; Bell, R.; Mootz, D. *Angew. Chem., Int. Ed. Engl.* **1998**, *37*, 3050.
(13) Drent, E.; Catharina, M.; De Kock, T. U.S. Patent 5,688,909, 1997.
(14) Shultz, C. S.; DeSimone, J. M.; Brookhart, M. *Organometeallics* **2001**, *20*, 16. Shultz, C. S.; DeSimone, J. M.; Brookhart, M. *J. Am. Chem. Soc.* **2001**, *123*, 9172.

10.1021/om011027+ CCC: $22.00
Publication on Web 04/06/2002

Scheme 1

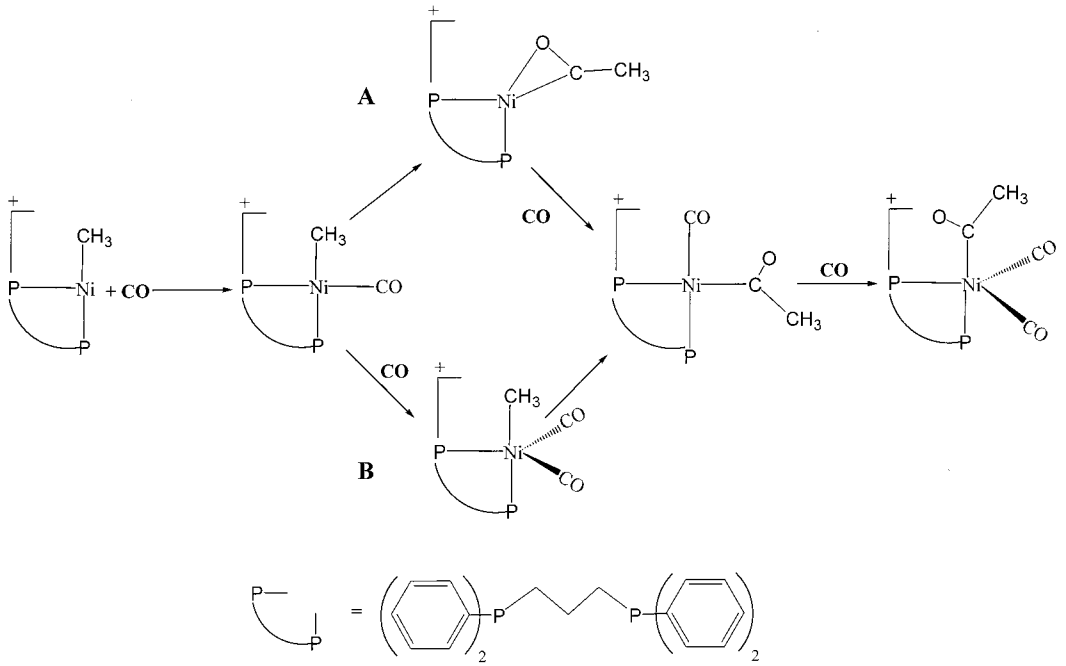

L)Ni(CH_3)(solv)]$^+$, L−L = dppp, and o-MeO-dppe with CO at −130 °C results in the immediate formation of five-coordinate acetyl dicarbonyl complexes [(L−L)Ni($COCH_3$)($CO)_2$]$^+$, indicating that the barrier to CO insertion must be less than or equal to ca. 10 kcal mol^{-1}. This behavior is in marked contrast to the reaction of the analogous palladium complexes, in which only four-coordinate acyl monocarbonyl complexes are observed and higher barriers for CO insertion are measured, such as 14.8 kcal mol^{-1} for [(dppp)Pd(CH_3)(CO)]$^+$.[7] In the o-MeO-dppe system, a five-coordinate methyl dicarbonyl complex [(o-MeO-dppe)Ni(CH_3)($CO)_2$]$^+$ species has been isolated which then undergoes the migratory insertion reaction. The identification of this species suggests that the reaction proceeds through the double carbonylation of [(L−L)Ni(CH_3)(solv)]$^+$ to the five-coordinate methyl dicarbonyl species, which then undergoes the migratory insertion and adds a further CO (path A in Scheme 1) rather than by the monocarbonylation of [(L−L)Ni(CH_3)(solv)]$^+$ to the four-coordinate methyl carbonyl species, which then undergoes the migratory insertion and adds two further CO (path B in Scheme 1).

Previous calculations on the CO insertion step in carbon monoxide olefin copolymerization have focused on the Pd(II) system,[15,16] and to the best of our knowledge only one theoretical work has been performed on cationic Ni(II) complexes by Morokuma and co-workers.[16] However, the diimine complex [(NH=CH−CH=NH))Ni(CH_3)(CO)]$^+$ with a bidentate nitrogen ligand has been addressed, and calculations have been performed only on four-coordinate species. To shed light on the mechanistic aspects of the migratory insertion in the cationic Ni(II) complexes with bidentate phosphine ligands, and in particular on the role played by five-coordinate species, we have carried out a theoretical study of the CO migratory insertion step in [(dppp)Ni(CH_3)(solv)]$^+$ by means of both static and dynamic density functional methods. The olefin insertion step will be the subject of a forthcoming paper.

For each of the two possible insertion pathways, proceeding via either a four-coordinate (path A) or a five-coordinate (path B) species, we have identified the equilibrium geometries and the relative energies for all the involved molecules and possible transition states, evaluating the overall energy profile. For path A and B we have also performed ab initio molecular dynamics (AIMD) simulations based on the Car−Parrinello approach[17] to study the hitherto inaccessible dynamic features of the insertion process.

Such a combination of static and dynamic DFT calculations has been already successfully employed in the study of similar CO migratory insertions.[18,19]

Results and Discussion

The initial step of the insertion reaction is supposed to be the addition of a CO molecule to the [(dppp)Ni(CH_3)(solv)]$^+$ species, which we initially modeled with a tricoordinate [(dpp)Ni(CH_3)]$^+$ complex, **1**, finding a T-shaped geometry with a vacant coordination site. We checked the relative energies of singlet and triplet states for this coordinatively unsaturated species, finding a singlet ground state with the triplet 23.6 kcal mol^{-1} higher in energy. Since for the considered tetra- and pentacoordinated complexes the triplet state is expected to be even higher in energy, we limited our analysis to the singlet potential energy surface.

We then optimized the geometry of the [(dpp)Ni(CH_3)(CO)]$^+$ complex, **2**, resulting from addition of a CO

(15) Margl, P.; Ziegler, T. *J. Am. Chem. Soc.* **1996**, *118*, 7337. Margl, P.; Ziegler, T. *Organometallics* **1996**, *15*, 5519. Koga, M.; Morokuma, K. *J. Am. Chem. Soc.* **1986**, *108*, 6136.

(16) Svensson, M.; Matsubara, T.; Morokuma, K. *Organometallics* **1996**, *15*, 5568.

(17) Car, R.; Parrinello, M. *Phys. Rev. Lett.* **1985**, *55*, 2471.

(18) De Angelis, F.; Re, N.; Sgamellotti, A.; Selloni, A.; Weber, J.; Floriani, C. *Chem. Phys. Lett.* **1998**, *291*, 57. De Angelis, F.; Sgamellotti, A.; Re, N. *J. Chem. Soc., Dalton Trans.* **2001**, 1023. Fantacci, S.; De Angelis, F.; Sgamellotti, A.; Re, N. *Organometallics* **2001**, *20*, 4031.

(19) De Angelis, F.; Sgamellotti, A.; Re, N. *Organometallics* **2000**, *19*, 4104.

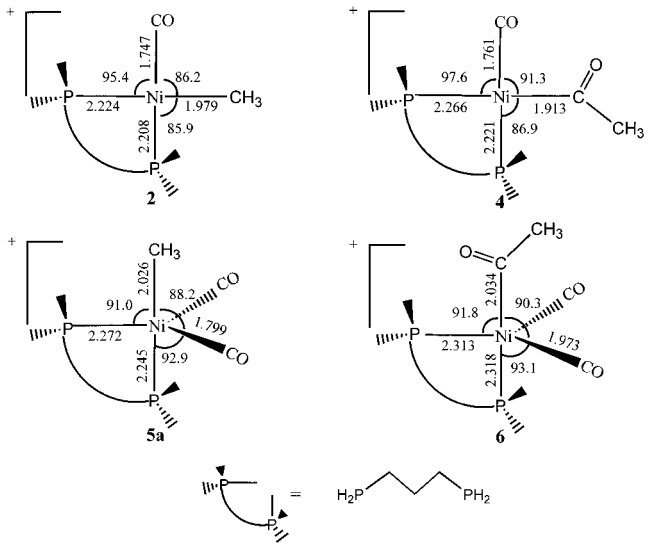

Figure 1. Structures and main optimized geometrical parameters (Å, deg) for complexes **2**, **4**, **5a**, and **6**.

molecule to **1**, finding a square-planar structure 30.2 kcal mol^{-1} below the energy of the free reagents. To provide a more realistic estimate of the energetics of the initial step, we also considered the ligand-exchange process leading from $[(dpp)Ni(CH_3)(H_2O)]^+$ to **2**, finding this process to be exothermic by 8.9 kcal mol^{-1}. The structure of **2**, together with main geometrical parameters, has been plotted in Figure 1.

Path A. Here we consider the direct migratory insertion in the four-coordinate complex **2**, followed by addition of a CO molecule to the incoming acyl species. Constrained AIMD simulations were performed, by means of the SHAKE algorithm,[20] starting from **2** by constraining the CH_3-CO distance to decrease from its initial value in **2**, ca. 2.58 Å, to its value in the tricoordinate acyl product **3a**, ca. 1.54 Å, as a function of the simulation time. The temperature of the nuclei is controlled by a Nosé thermostat[21] and fixed at 450 K.

By extracting selected configurations from the dynamics simulation and replacing phenyls with hydrogen atoms, we were able to locate the transition state, **TS$_{2\rightarrow 3a}$**, corresponding to the migratory insertion starting from **2**, finding a structure 11.3 kcal mol^{-1} higher than the reagent, in excellent agreement with the experimental value of 12.6 kcal mol^{-1}.[14] We then optimized the geometry of the product, an η^1-acyl intermediate stabilized by a CH_3-Ni agostic interaction, **3a**, finding it 4.6 kcal mol^{-1} higher than **2**. Such a local minimum is connected by a small energy barrier, less than 2 kcal mol^{-1}, to a more stable η^2-acyl isomer, **3b**, which was found 9.7 kcal mol^{-1} below **3a**, therefore 5.1 kcal mol^{-1} lower than **2**. This confirms the experimental assignment of an η^2-acyl structure to the acyl species in equilibrium with the tetracoordinate methyl-carbonyl complex **2**, based on low-temperature NMR data. Moreover, our results are consistent with the experimental evidence showing that the η^2-acyl complex **3b** is slightly more stable than **2**.

(20) Ryckaert, J.-P.; Ciccotti, G.; Berendsen, H. J. *J. Comput. Phys.* **1977**, *23*, 327.
(21) Nosè, S. *Mol. Phys.* **1984**, *52*, 255. Hoover, W. G. *Phys. Rev. A* **1985**, *31*, 1695.

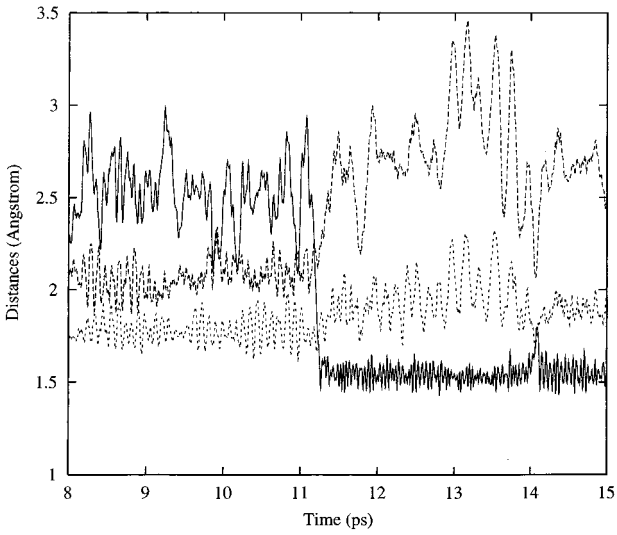

Figure 2. Time evolution of the CH_3-CO, solid line, CH_3-Ni, long-dashed line, and $Ni-C(CO)$, short-dashed line, distances (Å) for the dynamics simulation starting from the TBP complex **5a** for the time span 8−15 ps.

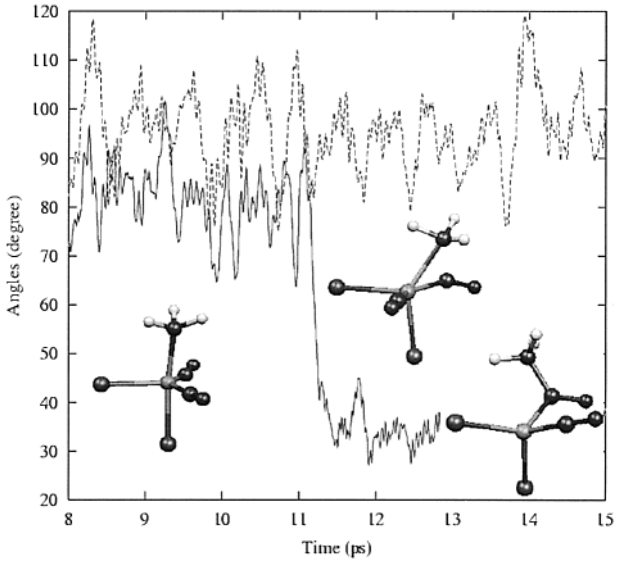

Figure 3. Time evolution of the $\angle CH_3-Ni-CO$, solid line, and axial $\angle P-Ni-CO$, long-dashed line, angles (deg) for the dynamics simulation starting from the TBP complex **5a** for the time span 8−15 ps, along with selected snapshots extracted from the AIMD run. The dppp ligand has been schematized by reporting only its P atoms.

The subsequent CO addition to **3b**, leading to a square-planar η^1-$[(dpp)Ni(CH_3CO)(CO)]^+$ acyl complex **4**, was found exothermic by 15.8 kcal mol^{-1}. The overall insertion−addition path A is therefore computed to be exothermic by 20.9 kcal mol^{-1}, with a highest energy barrier of 11.3 kcal mol^{-1}.

Path B. We then considered the addition of a CO molecule to **2** leading to a trigonal bipyramid (TBP) pentacoordinate $[(dpp)Ni(CH_3)(CO)_2]^+$ complex, **5**. To check whether a barrier to CO coordination exists, we performed a linear transit scan of the potential energy surface assuming the $Ni-C(CO)$ distance as a reaction coordinate, but no energy barrier was found for such a process. We then optimized the geometry of the possible TBP isomers of complex **5**, finding only two stable minima on the potential energy surface, corresponding

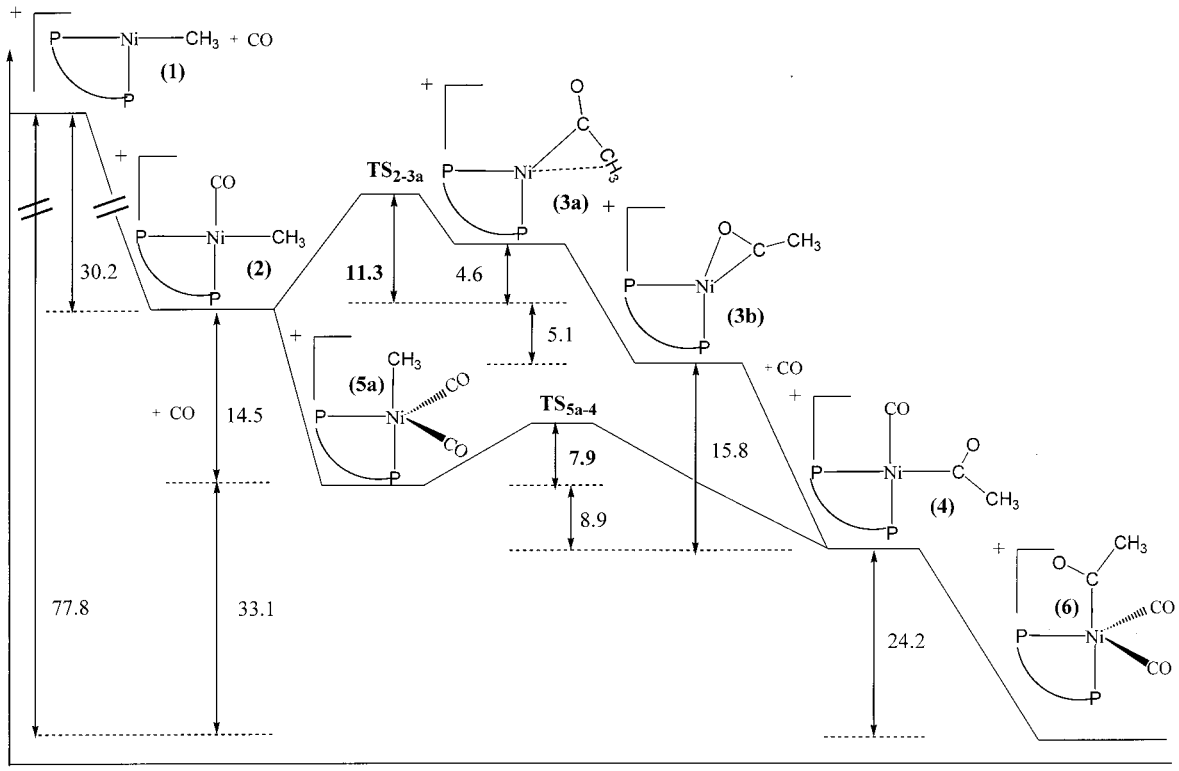

Figure 4. Schematic representation of the potential energy surface for the four-coordinate and five-coordinate reaction pathways leading to **6**. Energy in kcal mol^{-1}.

to axial CH_3 and P, **5a**, and axial CH_3 and CO, **5b**. The more stable isomer **5a** was found 14.5 kcal mol^{-1} below the energy of the free reagents (**2** + CO), with the **5b** isomer 4.3 kcal mol^{-1} above **5a**, in agreement with the trend already outlined for similar TBP complexes always showing axial preference for σ donor ligands.[19]

To gain some insight into the reaction mechanism of the migratory insertion process, we performed AIMD simulations by heating the structure of the more stable isomer **5a**. We did not apply any constraints to the nuclear coordinates, allowing all the degrees of freedom to evolve naturally in time; however, we used a higher temperature (450 K) than the experimental employed one (ca. 140 K) to speed up the reaction, so that we expect our simulation to provide qualitative insights into the reaction mechanism at the experimental temperature. Nevertheless, we had to extend the total time span of the simulation up to 15 ps.

The insertion evolution can be followed by studying the time evolution of the distance between the carbonyl and the methyl groups, the nickel−methyl and the nickel−carbonyl distances. Indeed, the CO−CH_3 distance is 2.61 Å in the reagent **5a**, in which the two carbons are part of two different ligands, while it is only 1.50 Å in the product **4**, where the two carbons are directly bonded; the Ni−CH_3 distance is 2.03 Å in **5a** and 3.07 Å in **4**. Figure 2 displays the variation of CO−CH_3, Ni−CH_3, and Ni−C(CO) distances as a function of the simulation time, for the time span going from 8 to 15 ps. From Figure 2 it appears that the reactive migration takes place after ca. 11 ps. Indeed, a fast decrease in the C−C distance from ca. 2.6 to ca. 1.5 Å is observed starting at 11 ps. Thereafter, the CO−CH_3 distance varies within the normal limits of C−C vibration. We can notice how the Ni−C distance follows an almost complementary trajectory with respect to the CO−CH_3 distance; nevertheless this distance shows higher oscillations, after 12 ps, due to the fact that at the end of the reaction the Ni and C atoms are no longer bound. Moreover, the CO group does not detach from the metal during the insertion reaction, as shown by the almost constant value of the Ni−C(CO) distance throughout the entire simulation time. To gain further insight into the reaction mechanism, we have analyzed the variation of the ∠CO−Ni−CH_3 and of the axial ∠P−Ni−CO bond angles, as a function of the simulation time, see Figure 3. The achievement of the migratory insertion is confirmed by the fast decrease in the ∠CO−Ni−CH_3 angle from its value of ca. 86° characteristic of **5a** to ca. 30° corresponding to **4**, observed around 11−12 ps. Moreover, we can notice that the insertion reaction is actually better described as a methyl attack on the resting carbonyl group; indeed the ∠P−Ni−CO bond angle does not show significant variations around 11−12 ps, in agreement with the experimental evidence.[22] Extracting selected configurations from the AIMD run and replacing phenyl groups with hydrogen atoms, we have been able to locate the transition state $\mathbf{TS_{5a\rightarrow 4}}$ for the conversion between **5a** and **4**, finding a structure 7.9 kcal mol^{-1} above **5a**, while no transition state connecting **5b** and **4** was found. We therefore see how the addition−insertion path B is an exothermic process by 23.4 kcal mol^{-1}, with a highest energy barrier of 7.9 kcal mol^{-1}, again in agreement with the experimental estimate, indicating a barrier lower than 10 kcal mol^{-1}. We finally optimized the geometry of the five-coordinate $[(dpp)Ni(COCH_3)(CO)_2]^+$ complex, **6**, result-

(22) Noack, K.; Calderazzo, F. *J. Organomet. Chem.* **1967**, *10*, 101. Atwood, J. D. *Inorganic and Organometallic Reaction Mechanisms*; Brooks/Cole Publishing Company: Monterey, CA, 1985.

ing from addition of a CO molecule to **4**, finding a TBP pentacoordinate structure 24.2 kcal mol^{-1} below **5a**. A schematic representation of the energy profile for both paths A and B can be found in Figure 4, while structures and main geometrical parameters for **2**, **4**, **5a**, and **6** can be found in Figure 1.

We therefore conclude that the addition−insertion path B, taking place via a five-coordinate complex, is the thermodynamically and kinetically favored pathway and is exothermic by 23.4 kcal mol^{-1}, with a highest energy barrier of 7.9 kcal mol^{-1}, in agreement with the experiment. AIMD simulations performed on this pathway have shown that the migratory insertion reaction takes place within 12 ps by a methyl attack on the resting carbonyl group.

Computational Details

Static DFT Calculations. The static DFT calculations reported in this paper have been performed using the Gaussian 98 program package[23] on a reduced model in which the phenyl groups of the dppp moiety have been replaced by hydrogens. We refer to such a model diposphine propane ligand as "dpp". We used a 6-311G* basis set[24−26] for all the atoms. Geometry optimizations were performed considering the Vosko−Wilk−Nusair LDA parametrization[27] and including the Becke[28] and Perdew−Wang[29] gradient corrections to the exchange and correlation, respectively. All stationary points were optimized without any symmetry constraints; frequency calculations have been performed on the computed transition state structures. To check the reliability of our model, we computed the thermodynamics of the five-coordinate migratory insertion reaction considering the real dppp ligand, using a 6-311g* basis set for all the atoms except the phenyl ligands, for which a 3-21g* basis was used, finding a negligible difference (8.9 vs 9.2 kcal mol^{-1}).

Car−Parrinello Calculations. AIMD simulations were carried out with the Car−Parrinello (CP) method[17,30] for path B using the real complex $[(dppp)Ni(CH_3)(CO)_2]^+$ to account for steric effects of the phenyl groups. Such a choice has been driven by the high computational efficiency of the CP method which allows the investigation of larger systems. For the LDA exchange−correlation functional the Perdew−Zunger parametrization[31] has been used, while the gradient-corrected functional is taken from ref 32. Core states are projected out using pseudopotentials. For Ni, C, and O "ultra-soft" pseudopotentials were generated according to the scheme proposed by Vanderbilt,[33] whereas for P the Hamann−Schluter−Chang (HSC) pseudopotential[34] has been used. The wave functions were expanded in plane waves up to an energy cutoff of 25 Ry. Periodic boundary conditions were used by placing the model molecule in a cubic box of 15.87 Å, sufficiently large to avoid coupling between periodic images. The equations of motion were integrated using a time step of 10 au (0.242 fs) with an electronic fictitious mass $\mu = 1000$ au.

Acknowledgment. Thanks are due to the CNR (Progetto Finalizzato "Materiali Speciali per Tecnologie Avanzate II") for financial support.

Supporting Information Available: Mpg movie of the dynamics simulation performed on path B. Optimized geometrical structures. This material is available free of charge via the Internet at http://pubs.acs.org.

OM011027+

(23) Frisch, M. J.; et al. *Gaussian 98* (Revision A.7); Gaussian, Inc.: Pittsburgh, PA, 1998.
(24) Frisch, M. J.; Pople, J. A.; Binkley, J. S. *J. Chem. Phys.* **1984**, *80*, 3265, and references therein.
(25) Hay, P. J. *J. Chem. Phys.* **1977**, *77*, 4377.
(26) Wachters, A. J. H. *J. Chem. Phys.* **1970**, *52*, 1033.
(27) Vosko, S. H.; Wilk, L.; Nusair, M. *Can. J. Phys.* **1980**, *58*, 1200.
(28) Becke, A. D. *Phys. Rev.* **1988**, *A38*, 3098.
(29) Perdew, J. P.; Wang, Y. *Phys. Rev.* **1992**, *B45*, 13244.
(30) The implementation that we use is decribed in: Pasquarello, A.; Laasonen, K.; Car, R.; Lee, C.; Vanderbilt, D. *Phys. Rev. Lett.* **1992**, *69*, 1982. Pasquarello, A.; Laasonen, K.; Car, R.; Lee, C.; Vanderbilt, D. *Phys. Rev. B* **1993**, *47*, 10142.
(31) Perdew, J. P.; Zunger, A. *Phys. Rev. B* **1981**, *23*, 5048.
(32) Perdew, J. P.; Chevary, J. A.; Vosko, S. H.; Jackson, K. A.; Pederson, M. R.; Singh, D. J.; Fiolhais, C. *Phys. Rev. B* **1992**, *46*, 6671.
(33) Vanderbilt, D. *Phys. Rev. B* **1990**, *41*, 7892.
(34) Hamann, D. R.; Schlüter, M.; Chiang, C. *Phys. Rev. Lett.* **1979**, *43*, 1494.